Supporting Information

Lindskog et al. 10.1073/pnas.1016399107

SI Text

Retrograde Messengers. We considered a number of molecules or molecular signaling systems, previously implicated in retrograde signaling at synapses, as potential candidates. Brain-derived neurotrophic factor (BDNF) is a leading possibility because it increases mini excitatory frequency in hippocampal neurons within minutes of exogenous application (1, 2), and can be released from a depolarized postsynaptic neuron (3, 4). Nitric oxide (NO) is another attractive candidate, which has been found to act as a retrograde messenger, capable of rapidly influencing presynaptic vesicle recycling (5, 6). Endocannabinoids have been firmly established as retrograde messengers at many synapses, and are released in response to rises in postsynaptic $[Ca^{2+}]_i$ (7, 8), but they inhibit glutamatergic neurotransmission (9, 10), in contrast to the enhancement sought here (1). Arachidonic acid (AA) has long been considered as a possible retrograde messenger at CNS synapses (11–13), but its ability to enhance excitatory postsynaptic potentials requires presynaptic stimulation (13), a constraint not found in our system (an increase in miniature excitatory postsynaptic current (mEPSC) frequency was seen within minutes, even with TTX present, Figs. 1–3) (2). *All-trans* retinoic acid (atRA) is another player in synaptic plasticity (14), with significant and interesting impact on homeostatic scaling (15); however, its known receptors and target actions are postsynaptic (3, 15). Tumor-necrosis factor alpha (TNF-α) has been implicated as a key factor in synaptic scaling, but it is released from glial cells, not postsynaptic neurons (5, 16). β-Catenin can interact with cadherin in postsynaptic targets, thereby increasing synaptic size, strength, and malleability (17). Although presynaptic consequences have been described (18), it is membrane depolarization that drives β-catenin accumulation in spines (19), making it unsuitable for explaining the slow inactivity-induced structural changes of concern here.

1. Li Y-X, Zhang Y, Lester HA, Schuman EM, Davidson N (1998) Enhancement of neurotransmitter release induced by brain-derived neurotrophic factor in cultured hippocampal neurons. *J Neurosci* 18:10231–10240.
2. Berninger B, Schinder AF, Poo MM (1999) Synaptic reliability correlates with reduced susceptibility to synaptic potentiation by brain-derived neurotrophic factor. *Learn Mem* 6:232–242.
3. Magby JP, Bi C, Chen Z-Y, Lee FS, Plummer MR (2006) Single-cell characterization of retrograde signaling by brain-derived neurotrophic factor. *J Neurosci* 26:13531–13536.
4. Moulder KL, Jiang X, Taylor AA, Olney JW, Mennerick S (2006) Physiological activity depresses synaptic function through an effect on vesicle priming. *J Neurosci* 26:6618–6626.
5. Micheva KD, Buchanan J, Holz RW, Smith SJ (2003) Retrograde regulation of synaptic vesicle endocytosis and recycling. *Nat Neurosci* 6:925–932.
6. Moulder KL, et al. (2004) Plastic elimination of functional glutamate release sites by depolarization. *Neuron* 42:423–435.
7. Safo PK, Regehr WG (2005) Endocannabinoids control the induction of cerebellar LTD. *Neuron* 48:647–659.
8. Carlson G, Wang Y, Alger BE (2002) Endocannabinoids facilitate the induction of LTP in the hippocampus. *Nat Neurosci* 5:723–724.
9. Gerdeman G, Lovinger DM (2001) CB1 cannabinoid receptor inhibits synaptic release of glutamate in rat dorsolateral striatum. *J Neurophysiol* 85:468–471.
10. Misner DL, Sullivan JM (1999) Mechanism of cannabinoid effects on long-term potentiation and depression in hippocampal CA1 neurons. *J Neurosci* 19:6795–6805.
11. Freeman EJ, Terrian DM, Dorman RV (1990) Presynaptic facilitation of glutamate release from isolated hippocampal mossy fiber nerve endings by arachidonic acid. *Neurochem Res* 15:743–750.
12. Schmidt JT, Fleming MR, Leu B (2004) Presynaptic protein kinase C controls maturation and branch dynamics of developing retinotectal arbors: Possible role in activity-driven sharpening. *J Neurobiol* 58:328–340.
13. Bliss TV, Errington ML, Lynch MA, Williams JH (1990) Presynaptic mechanisms in hippocampal long-term potentiation. *Cold Spring Harb Symp Quant Biol* 55:119–129.
14. Chiang MY, et al. (1998) An essential role for retinoid receptors RARbeta and RXRgamma in long-term potentiation and depression. *Neuron* 21:1353–1361.
15. Aoto J, Nam CI, Poon MM, Ting P, Chen L (2008) Synaptic signaling by all-trans retinoic acid in homeostatic synaptic plasticity. *Neuron* 60:308–320.
16. Stellwagen D, Malenka RC (2006) Synaptic scaling mediated by glial TNF-alpha. *Nature* 440:1054–1059.
17. Okuda T, Yu LMY, Cingolani LA, Kemler R, Goda Y (2007) β-Catenin regulates excitatory postsynaptic strength at hippocampal synapses. *Proc Natl Acad Sci USA* 104:13479–13484.
18. Li XM, et al. (2008) Retrograde regulation of motoneuron differentiation by muscle beta-catenin. *Nat Neurosci* 11:262–268.
19. Murase S, Mosser E, Schuman EM (2002) Depolarization drives beta-Catenin into neuronal spines promoting changes in synaptic structure and function. *Neuron* 35:91–105.
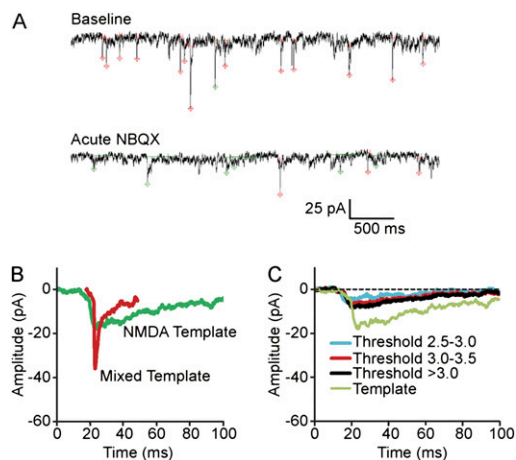
Fig. S1. Synaptic events were detected using a semiautomated template search (1), implemented in Clampfit 10.2. Standard templates for NMDA and mixed (NMDA + non-NMDA) events were created by averaging at least 10 mEPSCs in the respective categories. Every mini was counted as a unitary vesicular release event, regardless of whether it was detected by the NMDA template, by the mixed template, or by both. The focus of our study was on detection of presynaptic release, not on the nature of the mini. To maximize the joint coverage of the two templates in combination, the mixed template was deliberately oriented toward events dominated by a large AMPA component, which were easily detected because of their large amplitude and sharp rise. The criteria for minis lacking a large AMPA component were carefully optimized to maximize the sensitivity for detection while keeping false positives to a minimum. The quality of the detected traces can be seen by consideration of NMDA-only minis showing the loosest fits among those considered acceptable. The average of such events was virtually identical in amplitude and waveform to the average of all of the accepted events. (A) Representative traces before and after acute NBQX treatment (no chronic treatment with NBQX) showing the events detected by the template-match function in Clampfit 10.2. Detected events are marked by red and green symbols at their peaks. Red, detection by amplitude scaling of mixed event template; green, detection by scaling of NMDAR template. (B) NMDAR and mixed mini templates, generated by averaging at least 10 events. (C) Time-aligned averages of mEPSC events detected by the NMDAR template at varying levels of stringency (the higher the matching threshold parameter, the higher the stringency). Comparison of all accepted events (matching threshold >3.0) with a subset of the accepted events, detected with minimal stringency (matching threshold between 3.0 and 3.5) and with rejected events (matching threshold between 2.5 and 3.0).
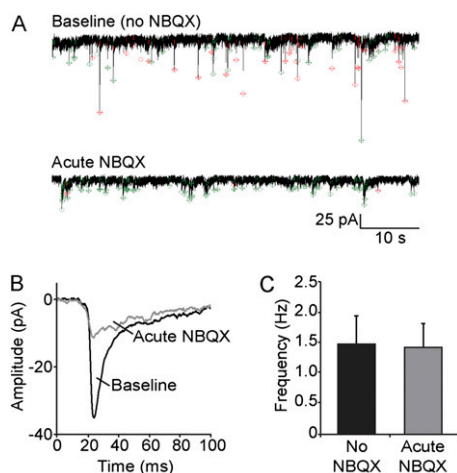
Fig. S2. The effectiveness of the detection strategy can be judged by the ability to detect NMDA minis with reliability comparable to that for mixed events including a substantial AMPA component. We tested this empirically in control experiments where minis were recorded in the absence and acute presence of AMPAR blocker. With both AMPA and NMDA receptors in operation, the minis typically displayed a sharp, high amplitude peak due to AMPA receptor opening, and a slow, low-amplitude decay phase due to NMDA receptor opening. In NBQX, the large, fast events were largely eliminated, leaving an average mini waveform that was almost entirely slow, low-amplitude NMDA current. The disappearance of the sharply peaking component is as expected for AMPAR-mediated current. It is also noteworthy that the remaining NMDA current is close to the same size as the slow component of the mixed GluR mini. If there had been a significant shortfall in the detection of NMDAR-only minis, allowing the smallest events to escape detection, the average would have been skewed in favor of bigger NMDA events. In contrast, the mixed GluR current, which is easy to detect, would contain a slow component indicative of the true size of the NMDA current. In fact, the slower component of the mixed GluR current was not smaller than the NMDA-only minis, indicating that the detection of NMDAR-dominated minis is comparably sensitive to that for mixed events. Further indication of the reliability of detection was provided by comparing the rate of spontaneous mEPSCs before and after acute AMPAR blockade. The mini frequency averaged 1.4 ± 0.4 Hz after acute NBQX application, not significantly different from the preapplication average of 1.5 ± 0.5 Hz ($P > 0.7$ by paired t test, $n = 6$). (A) Representative 60-s recordings from a hippocampal neuron before (baseline, 74 detected events) and after acute NBQX treatment (75 detected events). Peaks of mEPSC events detected using NMDA or mixed templates are marked, respectively, with green and red symbols. (B) Averaged records derived from time alignment of all detected events in the two traces in A. Acute NBQX treatment causes a marked attenuation of the kinetically fast AMPAR-dependent component (gray trace). The amplitude of the slow component (NMDAR current) is no different in acute NBQX relative to baseline conditions (black trace). (C) Pooled data for the frequency of mEPSCs before (black) and after acute NBQX application (gray) ($n = 6$). There is no significant change in mini frequency ($P = 0.74$ by paired t test, $n = 6$).
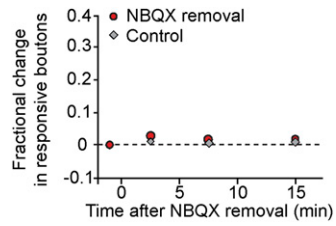
Fig. S3. Synaptic adaptation to hyperactivity can involve dramatic changes in the percentage of boutons that are presynaptically silent (5, 7). This prompted us to examine the proportion of nerve terminals that were silent as opposed to responsive in the form of synaptic adaptation studied here. Fig. S3 graph shows relative changes in the proportion of responsive boutons, determined in individual fields of view, using a level of >3 SD of baseline noise as the detection threshold. The change in the proportion of responsive boutons was less than 3% over the course of the NBQX removal and displayed no significant difference between chronic NBQX-treated and control groups at any time point (see Fig. 3 legend for details). Thus, the proportion of presynaptically active synapses provided little or no contribution to the overall change in the probability of release in this form of synaptic adaptation.